

# FEM Investigation of a Multi-Neck Helmholtz Resonator

Nikolaos M. Papadakis<sup>1,2,\*</sup>  and Georgios E. Stavroulakis<sup>1</sup> 

<sup>1</sup> Institute of Computational Mechanics and Optimization (Co.Mec.O), School of Production Engineering and Management, Technical University of Crete, 73100 Chania, Greece; gestavroulakis@tuc.gr

<sup>2</sup> Department of Music Technology and Acoustics, Hellenic Mediterranean University, 74100 Rethymno, Greece

\* Correspondence: nikpapadakis@tuc.gr

**Abstract:** An increasingly significant area of research with several applications in numerous disciplines is that of multi-neck Helmholtz resonators. This research is set to explore the accuracy and applicability of the finite element method (FEM) for the calculation of the resonance frequency of multi-neck Helmholtz resonators. The FEM is employed for the estimation of the resonance frequency in various cases of multi-neck Helmholtz resonators: with cylindrical or spherical bodies, with unflanged or flanged necks of various dimensions and with various combinations of the above. Also, single neck resonators are examined. The FEM results are compared with the results of a recently proposed theoretical model available in the literature and with the outcome of the lumped element approximation (multi-neck) accounting for the added neck surface area. Comparisons revealed little deviation between the FEM and theoretical model (less than 1.1% error of calculation for every case). On the contrary, in comparison with the lumped element approximation (multi-neck), the error of calculation is significant (up to 40.3% for the cases examined). The FEM will prove useful in expanding our understanding of how multi-neck Helmholtz resonators perform under various conditions and configurations. The present research, which highlights the applicability of the FEM for the calculations of the resonance frequency of multi-neck Helmholtz resonators, goes a step further; this approach can be applied in special cases where it is not trivial to apply an analytical formula. The method can be used for applications of multi-neck Helmholtz resonators for various fields such as acoustic metamaterials, musical acoustics and noise mitigation.

**Keywords:** Helmholtz resonator; multi-neck Helmholtz resonator; finite element method; leakage; absorption; acoustic transmission



**Citation:** Papadakis, N.M.; Stavroulakis, G.E. FEM Investigation of a Multi-Neck Helmholtz Resonator. *Appl. Sci.* **2023**, *13*, 10610. <https://doi.org/10.3390/app131910610>

Academic Editor: Lamberto Tronchin

Received: 1 September 2023  
Revised: 17 September 2023  
Accepted: 22 September 2023  
Published: 23 September 2023



**Copyright:** © 2023 by the authors. Licensee MDPI, Basel, Switzerland. This article is an open access article distributed under the terms and conditions of the Creative Commons Attribution (CC BY) license (<https://creativecommons.org/licenses/by/4.0/>).

## 1. Introduction

Helmholtz resonance is known as the phenomenon of air resonating in a cavity, as when one blows over the top of an empty bottle. A container with a small neck and a known volume constitutes the basic building block of a Helmholtz resonator. The compressible fluid in the resonator functions as a spring in the limit when the acoustic frequency is so low that the wavelength is much bigger than any dimension of the resonator [1]. Another parallelism that is used in the literature is that the fluid in the neck serves as an inductor (or mass), while the liquid volume serves as a capacitor (or spring) [2].

Numerous applications of the Helmholtz resonator can be found in the literature. Helmholtz resonators can be used to control noise in aircrafts [3], with the purpose of reducing a duct's transmission loss [4] and mitigating the noise of engines [5] and gas turbines [6]. In addition, Helmholtz resonators can be used for room acoustics, with applications as sound absorbers [7,8], changing the acoustic behavior of the space which can be evaluated with a suitable source [9–11] and signal [12]. They have also been used for the same purpose in churches [13] and ancient theaters [14]. Helmholtz resonators can also be used for environmental noise control, increasing the effectiveness of noise barriers [15–17]. It is also quite common for the Helmholtz resonance to be exploited in the manufacture of bass reflex for speakers [18]. The Helmholtz resonator has extensive

application in the study of musical acoustics [19]. The sound of the lowest notes, which are frequently below the frequencies of the lowest strongly excited, acoustically effective, structural resonances, is amplified by a Helmholtz air resonance in almost all hand-held stringed instruments and many bigger ones, such as the concert harp [1]. More recent uses of the Helmholtz resonator can be found in the field of acoustic metamaterials with applications for transmission loss [20], sound absorption [21], as an acoustic superlens [22] or as an ultrasonic metamaterial [23]. In addition, artificial neural networks have been used for the simulation of acoustic properties of resonators [24]. Finally, it can also be used for acoustic energy harvesting [25].

As was previously mentioned, a Helmholtz resonator typically consists of a container with a small neck and a specified volume. However, several modifications in the Helmholtz resonator's design and form have been researched in the literature. For instance, considering the resonator's neck form, variations have been examined such as with a spiral neck [26], with a tapered neck [27], with an extended neck [28] or with an angled neck aperture [29]. Accordingly, variations have been explored regarding the shape of the container [30,31]. Finally, there are several variations regarding the connection of the parts of the resonator, e.g., neck–cavity–neck–cavity (Dual Helmholtz resonator) [32].

An interesting variation, and also an interesting area of research, is that in which the resonator has more than one neck (usually called multi-neck Helmholtz resonator [33]). The same phenomena is discernible in a situation where there is a leak or a gap in the Helmholtz resonator, which, in this case, can also be called the leakage effect in Helmholtz resonators [34]. Selamet et al. [34] have examined the impact of leaks and gaps (i.e., extra necks) in Helmholtz resonators using experimental and computational methods. They noticed that as more necks are added to a Helmholtz resonator's internal baffle, the resonance frequency rises. A similar result is seen when the necks are placed on the resonator's outside surface [35]. Since manufacturing tolerances make it impossible to prevent leaks or gaps in Helmholtz resonators in many real-world applications [34], or perhaps require, for example, drainage of moisture that has accumulated inside the cavity [36], the effect of several necks on Helmholtz resonators must be understood and taken into consideration.

A novel analytical methodology to determine the resonance frequency of a Helmholtz resonator with numerous necks was developed in a recent work by Langfeldt et al. [33]. The resonance frequency is calculated by the model using a lumped representation of the air volumes encircled by the necks. Impedance tube measurements and experimental data from the literature were used to validate the results of the analytical model. Unlike the comprehensive multi-dimensional boundary element model (BEM) of Selamet et al. [34], an explicit formula for the resonance frequency of such resonator configurations was presented using the proposed model. Therefore, it may be used to calculate the effects of many necks (caused, for example, by leaks) in various Helmholtz resonator layouts.

Computational methods can be exploited for the study of multi-neck Helmholtz resonators, as previously demonstrated by Selamet et al. [34] utilizing a BEM. Among computational methods, the FEM is probably the most widely used in acoustic problems and has been applied for noise control [37], in architectural and environmental acoustics [38] and also in the frequency and time domain [39,40]. This work seeks to evaluate the efficacy and usability of the FEM for the determination of the resonance frequency of multi-neck Helmholtz resonators. For this purpose, results will be compared between the FEM and the results of the Langfeldt et al. [33] analytical model for various cases of Helmholtz resonators with multiple necks.

The structure of this paper is as follows: The methodology is described in Section 3. The research's results are presented in Section 4, while the Section 5 examines the data, responds to the research question, and suggests topics for future study. A brief overview of this research is provided in the Section 6, which also places the work in its larger perspective.

## 2. Background

In this section, background information will be presented on the three different ways the resonance frequency was calculated for the Helmholtz resonator: Langfeldt et al.'s [33] theoretical formulation; FEM; Lumped-element approximation.

### 2.1. Langfeldt et al. [33] Theoretical Formulation

In their work, to provide a theoretical formula for a multi-neck Helmholtz resonator's resonance frequency, Langfeldt et al. [33] considered that the fluid is compressed due to the volume change inside the cavity, creating a pressure amplitude that may differ significantly from the pressure amplitude outside the cavity, given that the acoustic wavelength at the resonance frequency is lower than the Helmholtz resonator cavity's dimensions. Consequently,  $p_0$  may be determined using the fluid's bulk modulus under the assumption that the pressure inside the cavity is uniform [41]. After a mathematical process, they arrived at the following formula for the resonance frequency of a Helmholtz resonator with multiple necks:

$$f_0 = \frac{c_0}{2\pi} \sqrt{\frac{\rho_0}{V_0} \sum_{i=1}^N \frac{S_i}{M_i}} \quad (1)$$

where  $c_0$  and  $\rho_0$  are the speed of sound and density of the fluid inside the cavity and  $V_0$  is the cavity volume. A total of  $N$  necks attached to the cavity, each neck  $i$ , with  $1 \leq i \leq N$ .  $S_i$  is the cross-sectional area of each neck. Finally,  $M_i$  can be interpreted as the inertial mass of the neck air volume. For cylindrical necks with diameter  $d_i$ , the neck air volume mass  $M_i$  is approximately:  $M_i = \rho_0(l_i + a_i d_i)$ . Taking into consideration the inertia of a certain fluid volume surrounding the neck,  $a_i$  is the so-called end correction coefficient and  $l_i$  is the neck length [34]. The end correction coefficient accounts for the 'induced mass' in the oscillatory flow in the vicinity of the two ends of the neck [42]. Values for the end correction coefficient can be found in various manuscripts. For a circular aperture, the end correction is  $a_i = \pi/4$  ( $\approx 0.785$ ) [43] or 0.75 for an unflanged pipe [44] and 0.85 for a flanged pipe [44].

Adding the resonance frequencies that correspond to the Helmholtz resonance frequencies allows Equation (1) to be written in a more condensed form, with all, except the  $i$ -th, openings closed. Therefore, Equation (1) becomes:

$$f_i = \frac{c_0}{2\pi} \sqrt{\frac{\rho_0}{V_0} \frac{S_i}{M_i}} \quad (2)$$

$$f_{leaks} = \frac{c_0}{2\pi} \sqrt{\frac{\rho_0}{V_0} \sum_{i=2}^N \frac{S_i}{M_i}} \quad (3)$$

$$f_0 = \sqrt{\sum_{i=1}^N f_i^2} = \sqrt{f_1^2 + f_{leaks}^2} \quad (4)$$

According to Equation (4), the resonance frequency of a Helmholtz resonator with multiple necks is given by the square root of the sum of the squared resonance frequency without leaks  $f_1^2$  and the squared resonance frequency with leaks only ( $f_{leaks}^2$ ).

### 2.2. FEM Formulation and Setup

In the Helmholtz equation,  $p$  stands for the acoustic pressure,  $\Delta$  for the Laplacian operator and  $k$  for the wave number.

$$\Delta p(\mathbf{x}) + k^2 p(\mathbf{x}) = 0 \quad (5)$$

According to the following equation, the normal derivative of the acoustic pressure  $p$  is associated with the normal fluid particle velocity  $u_f$ :

$$u_f(\mathbf{x}) = \frac{1}{i\omega\rho_f} \frac{\partial p(\mathbf{x})}{\partial n(\mathbf{x})} \tag{6}$$

In this equation,  $n(\mathbf{x})$  is the outward normal vector at a field point  $\mathbf{x}$  and  $\rho_f$  is the average density of the fluid.

As a next step, a weak formulation with weighting function  $\chi(\mathbf{x})$  was used, and the equation is formed as follows [45]:

$$\begin{aligned} & \int_{\Omega} \chi(\mathbf{x}) (\Delta p(\mathbf{x}) + k^2 p(\mathbf{x})) d\Omega(\mathbf{x}) \\ &= \int_{\Gamma} \chi(\mathbf{x}) i\omega\rho_f u_f(\mathbf{x}) d\Gamma(\mathbf{x}) + \int_{\Omega} (\nabla\chi(\mathbf{x})\nabla p(\mathbf{x}) - k^2\chi(\mathbf{x})p(\mathbf{x})) d\Omega(\mathbf{x}) = 0 \end{aligned} \tag{7}$$

In this notation,  $\Omega$  and  $\Gamma$  are the domain and boundary, respectively. Therefore, the acoustic pressure and particle velocity are shown as follows [45]:

$$\begin{aligned} p(\mathbf{x}) &= \sum_{n=1}^N \Phi_n(\mathbf{x}) p_n \\ u_f(\mathbf{x}) &= \sum_{n=1}^N \Phi_n(\mathbf{x}) u_n \end{aligned} \tag{8}$$

Finally,  $\Phi_n(\mathbf{x})$  is a basis function and  $p_n$  and  $u_n$  are the discrete acoustic pressure and fluid particle velocity at point  $\mathbf{x}$ . Adding Equation (9) to Equation (8) [45]:

$$(\mathbf{K} - ik\mathbf{C} - k^2\mathbf{M})\mathbf{p} = \mathbf{f} \tag{9}$$

$\mathbf{K}$ ,  $\mathbf{C}$  and  $\mathbf{M}$  are the stiffness, damping and mass matrices. Vector  $\mathbf{f}$  accounts for the source and vector  $\mathbf{p}$  accounts for the sound pressure values at the nodal locations.

### 2.3. Lumped-Element Approximation (Single Neck, Multi-Neck)

For a single neck Helmholtz resonator, according to the lumped element approximation [46], the resonance frequency can be estimated as (using nomenclature from Langfeldt et al. [33]):

$$f_0 = \frac{c_0}{2\pi} \sqrt{\frac{\rho_0 S_1}{V_0 M_1}} \tag{10}$$

where  $c_0$  and  $\rho_0$  are the speed of sound and density of the fluid inside the cavity and  $V_0$  is the cavity volume.  $S_1$  is the cross-sectional area of each neck. Finally,  $M_1$  (as presented in Section 2.1) can be seen as the inertial mass of the neck air volume. In the case of a cylindrical neck with diameter  $d_1$  and length  $l_1$ , the neck air volume mass  $M_1$  can be approximated as:  $M_1 = \rho_0(l_1 + a_1 d_1)$ .

For multi-neck Helmholtz resonators, both in the studies by Langfeldt et al. [33] and Selamet et al. [34], calculations were performed to account for the additional necks by simply combining the surface areas of the extra necks ( $S_2$ ) to that of the primary neck. For these calculations, the common lumped element approximation formula was expanded to accommodate for these changes. According to this approach, the fundamental acoustic resonant frequency can be calculated as (using nomenclature found in Langfeldt et al. [33]):

$$f_0 = \frac{c_0}{2\pi} \sqrt{\rho_0 \frac{S_1 + N_{leaks} S_2}{V_0 M_1}} \tag{11}$$

### 3. Methodology

In order to investigate the effectiveness of the FEM for the calculation of the resonance frequency of a Helmholtz resonator, different cases were considered in the methodology. Initially, single-necked Helmholtz resonators were modeled (spherical body, cylindrical

body) and compared with the results of the lumped element approximation formula (single-neck) and with the Langfeldt et al. [33] theoretical formulation. The reason for this approach is to confirm that our FEM modeling results are in line with the literature determining a (single-neck) Helmholtz resonator's resonance frequency (e.g., [47]). The above would be an indication that our single-neck models are structured correctly, behave as expected and are a good starting base for modeling of the multi-neck Helmholtz resonators, as in this case the literature is not as extensive. Next, various models of multi-neck Helmholtz resonators were tested to assess the effectiveness and applicability of the FEM for calculating the resonance frequency. The cases that were tested were a resonator with a spherical body with identical necks, a resonator with a cylindrical body with identical necks, a resonator with a spherical body with different necks, a resonator with a cylindrical body with different necks and finally a resonator with a cylindrical body with different necks and one flanged neck. Again, results were compared with the Langfeldt et al. [33] and the lumped element approximation formula.

For the estimation of the resonance frequencies in the case of Langfeldt et al.'s [33] theoretical formulation, Equation (4) was utilized. Accordingly, for the lumped-element approximation approach (single neck, multi-neck), Equations (10) and (11) were used, respectively. For all formulae, the speed of sound was set to 343 m/s and the density of air to  $\rho = 1.2 \text{ kg/m}^3$ . For all calculations, the end correction coefficient was set to 0.75 [44] (unflanged neck) and 0.85 [44] (flanged neck). For the calculations, the software Matlab R2021a (Mathworks, MA, USA) was used.

For the implementation of the FEM formulation as presented in Section 2.2., the commercial Comsol Multiphysics v.6.0 software (Comsol inc., Burlington, NJ, USA) was used. For the creation of the 3D models of the multi-neck Helmholtz resonators, the software Inventor v.2024 (Autodesk, San Francisco, CA, USA) was utilized. The general rule of thumb  $\lambda/h = 5$  was used to create the mesh, where  $\lambda$  and  $h$ , respectively, stand for the wavelength of the upper limit frequency and the maximum nodal distance. For acoustic modeling, five elements per wavelength were utilized, as is customary in the frequency domain [48]. A quadratic Lagrange triangular unstructured mesh was used to discretize the domain. For all FEM models, the speed of sound was set to 343 m/s and the density of air to  $\rho = 1.2 \text{ kg/m}^3$ .

## 4. Results

The results are presented in two categories below: single-neck models and multi-neck models.

### 4.1. Single-Neck Models

#### 4.1.1. Spherical Body

Initially, a single-neck Helmholtz resonator with a spherical body and cylindrical neck was considered (Figure 1). The tube radius of the neck of the resonator was  $a = 0.01 \text{ m}$ , the tube length was  $L = 0.06 \text{ m}$  and the volume radius of the resonators body was  $R_v = 0.06 \text{ m}$ . The acoustic pressure in the volume of the Helmholtz resonator was calculated with the FEM. Additionally, the resonance frequency according to the lumped-element approximation (single-neck) was calculated. The resonance frequency calculated with the FEM was 123.7 Hz and with the lumped-element approximations was 123.8 Hz (Figure 2). Figure 1 presents the acoustic pressure and the sound pressure level in the volume of the resonator for the resonance frequency.

#### 4.1.2. Cylindrical Body

For the second case, a single-neck Helmholtz resonator with a cylindrical body and a cylindrical neck was considered (Figure 3). The tube radius of the neck was  $a = 0.01 \text{ m}$  and the tube length was  $L = 0.05$ . Regarding the body of the resonator, the cylinder radius was 0.05 m and the cylinder height was 0.1 m. The acoustic pressure in the volume of the Helmholtz resonator was calculated with the FEM. Additionally, the resonance

frequency according to the lumped-element approximation (single-neck) was calculated. The resonance frequency calculated with the FEM was 144.0 Hz and with the lumped-element approximations was 144.0 Hz (Figure 4). Figure 3 presents the acoustic pressure and the sound pressure level in the volume of the resonator for the resonance frequency.

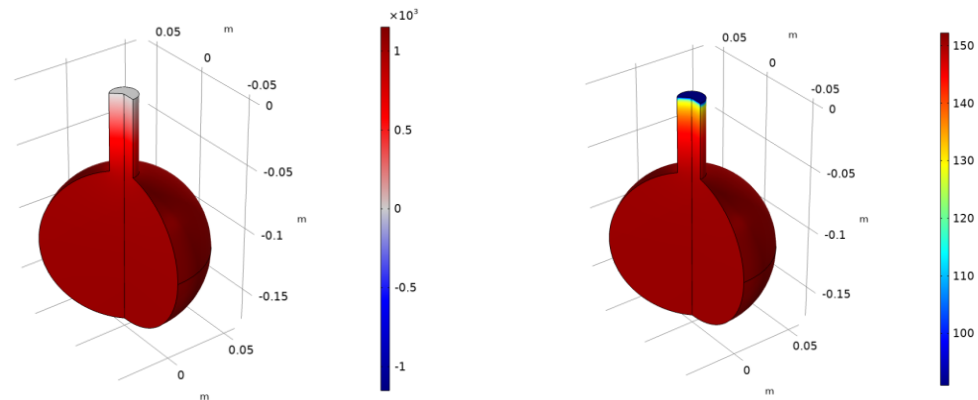


**Figure 1.** Acoustic pressure (left) (Pa) and sound pressure level (right) (dB) for the resonance frequency calculated with FEM (123.7 Hz).

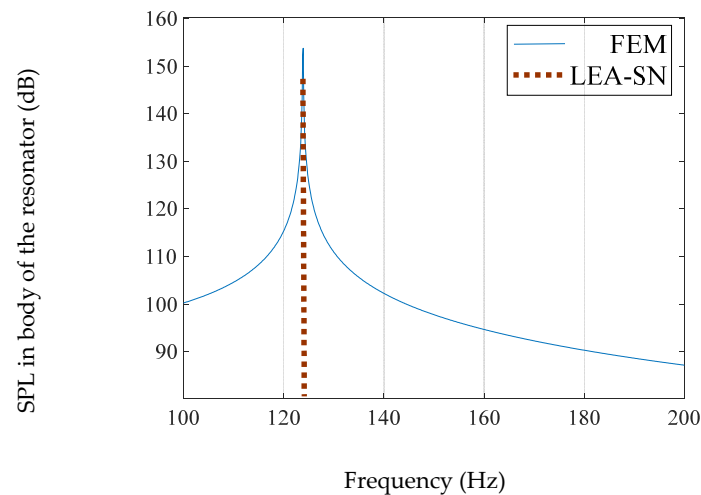


**Figure 2.** Solid line: sound pressure level in the body of the Helmholtz resonator calculated with FEM. Dotted line: resonance frequency calculated with lumped element approximation (single-neck).

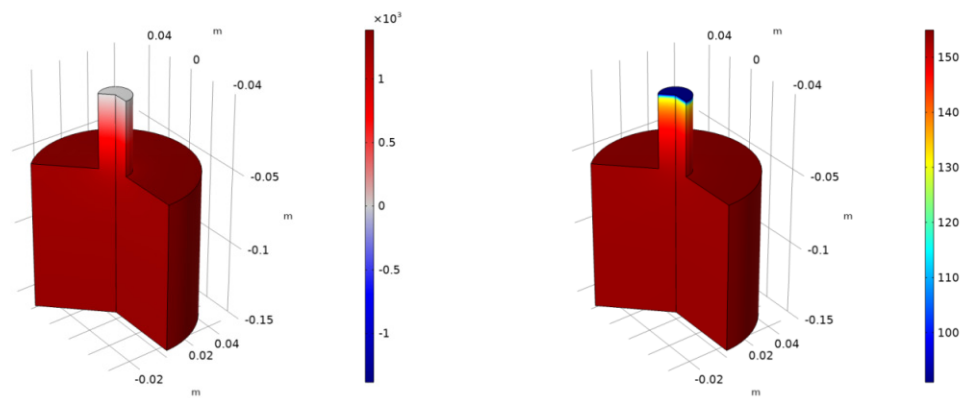


**Figure 3.** Acoustic pressure (left) (Pa) and sound pressure level (right) (dB) for the resonance frequency calculated with FEM (144.0 Hz).

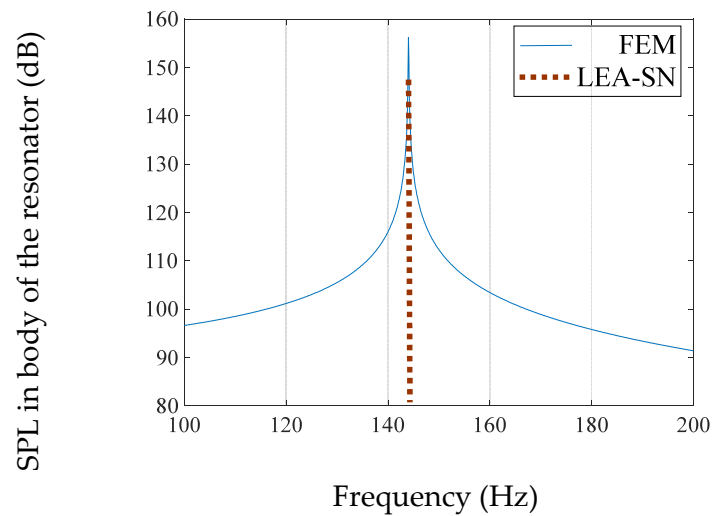


**Figure 4.** Solid line: sound pressure level in the body of the Helmholtz resonator calculated with FEM. Dotted line: resonance frequency calculated with lumped element approximation (single-neck).

#### 4.2. Multi-Neck Models

##### 4.2.1. Spherical Body #1 (Identical Necks)

For multi-necked Helmholtz resonators, several cases were considered. Initially, a multi-neck Helmholtz resonator with a spherical body and two identical cylindrical necks was considered (Figure 5). The tube radius of the necks was  $a = 0.01$  m, the tube length was  $L = 0.05$  m and the volume radius of the resonators body was  $R_v = 0.05$  m. The FEM was used to compute the acoustic pressure within the Helmholtz resonator's volume. Additionally, the resonance frequency was calculated according to the lumped-element approximation (multi-neck) and according to Langfeldt et al.'s [33] theoretical formulation. The resonance frequency calculated with the FEM was 249.7 Hz, with the lumped-element approximations was 249.4 Hz and with the Langfeldt et al. [33] theoretical formulation was 249.4 (Figure 6). Additionally, shown in Figure 5 are the acoustic pressure and sound pressure levels for the resonance frequency in the resonator's volume.

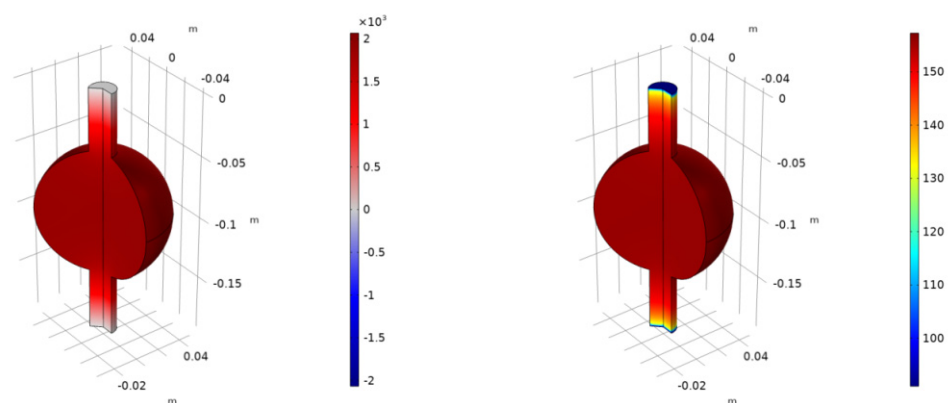


**Figure 5.** Acoustic pressure (left) (Pa) and sound pressure level (right) (dB) for the resonance frequency calculated with FEM (249.7 Hz).

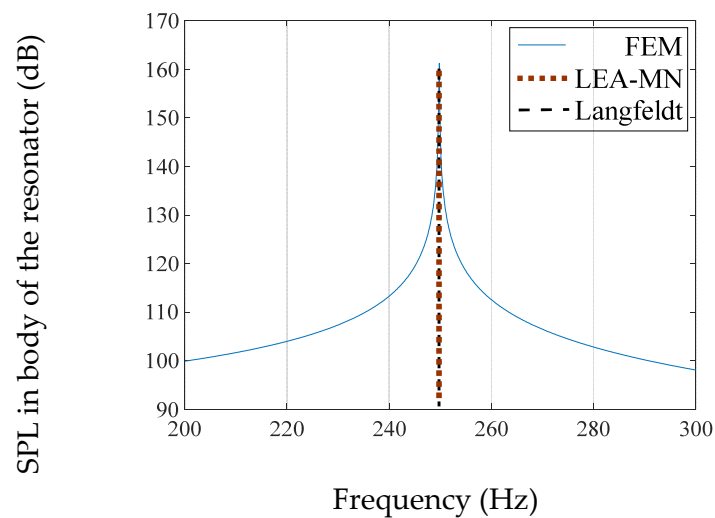


**Figure 6.** Solid line: sound pressure level in the body of the Helmholtz resonator calculated with FEM. Dotted line: resonance frequency calculated with lumped element approximation (multi-neck). Dashed line: resonance frequency calculated with Langfeldt et al.'s [33] formula.

#### 4.2.2. Cylindrical Body #1 (Identical Necks)

For the second case, a multi-neck Helmholtz resonator with a spherical body and two identical cylindrical necks was considered (Figure 7). The tube radius of the neck was  $a = 0.01$  m and the tube length was  $L = 0.05$ . Regarding the body of the resonator, the cylinder radius was 0.05 m and the cylinder height was 0.1 m. The FEM was used to compute the acoustic pressure within the Helmholtz resonator's volume. Additionally, the resonance frequency was calculated according to the lumped-element approximation (multi-neck) and according to Langfeldt et al.'s [33] theoretical formulation. The resonance frequency calculated with the FEM was 204.3 Hz, with the lumped-element approximations (multi-neck) was 203.6 Hz and with the Langfeldt et al. [33] theoretical formulation was 203.6 (Figure 8). Additionally, shown in Figure 7 are the acoustic pressure and sound pressure levels for the resonance frequency in the resonator's volume.

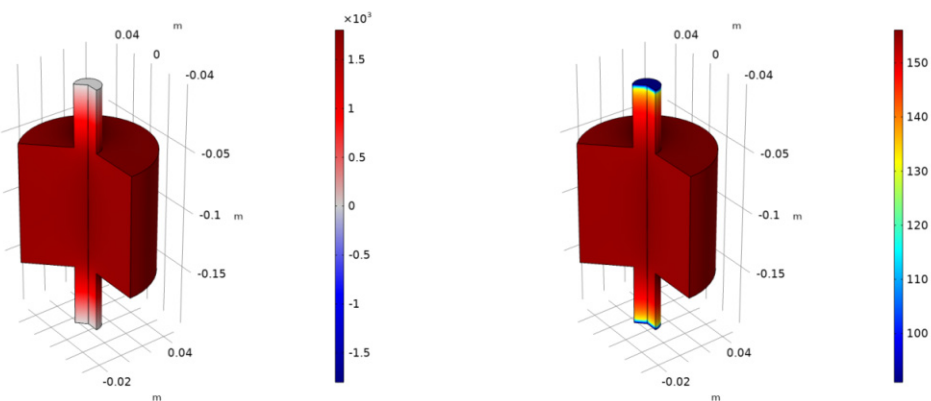


**Figure 7.** Acoustic pressure (left) (Pa) and sound pressure level (right) (dB) for the resonance frequency calculated with FEM (204.3 Hz).

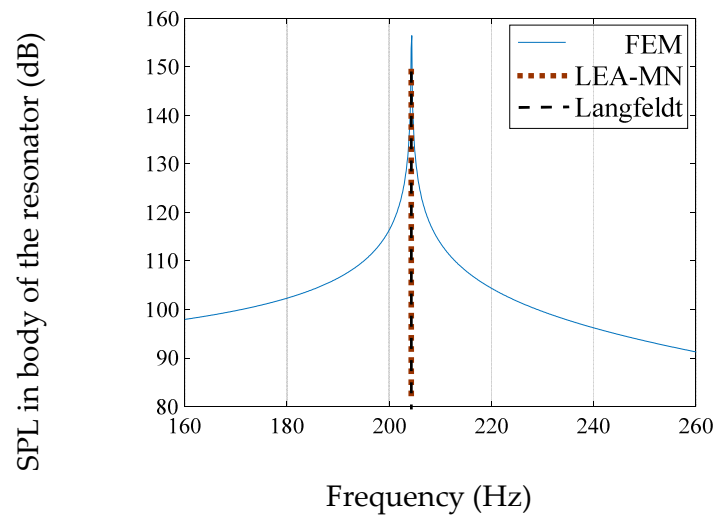


**Figure 8.** Solid line: sound pressure level in the body of the Helmholtz resonator calculated with FEM. Dotted line: resonance frequency calculated with lumped element approximation (multi-neck). Dashed line: resonance frequency calculated with Langfeldt et al.'s [33] formula.

#### 4.2.3. Spherical Body #2 (Different Necks)

In this case, a multi-neck Helmholtz resonator with a spherical body and two cylindrical necks with different dimensions was considered (Figure 9). The tube radius of the first neck was  $a = 0.01$  m and the tube length was  $L = 0.05$  m. The tube radius of the second neck was  $a/4$  and the tube length was  $L/4$ . The volume radius of the resonator's body was  $R_v = 0.05$  m. The acoustic pressure in the volume of the Helmholtz resonator was calculated with the FEM. In addition, the lumped-element approximation was used to obtain the resonance frequency (multi-neck) and also according to Langfeldt et al.'s [33] theoretical formulation. The resonance frequency calculated with the FEM was 199.3 Hz, with the lumped-element approximations (multi-neck) was 181.8 Hz and with the Langfeldt et al. [33] theoretical formulation was 197.1 Hz (Figure 10). The sound pressure level and acoustic pressure for the resonance frequency are also shown in Figure 9 for the resonator's volume.

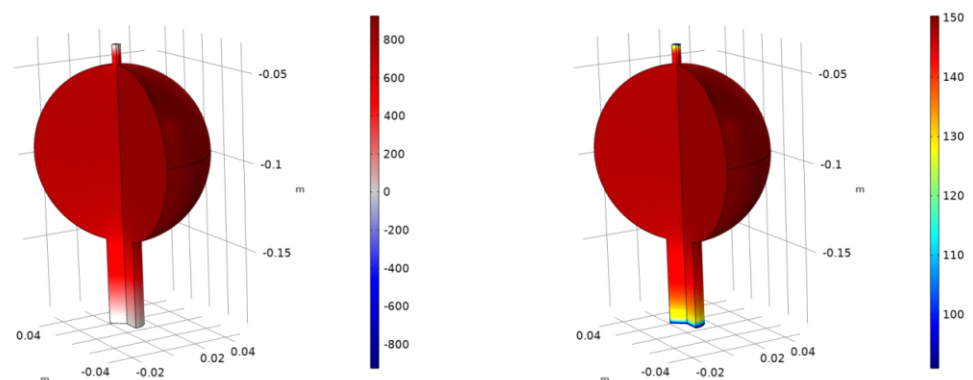


**Figure 9.** Acoustic pressure (left) (Pa) and sound pressure level (right) (dB) for the resonance frequency calculated with FEM (199.3 Hz).

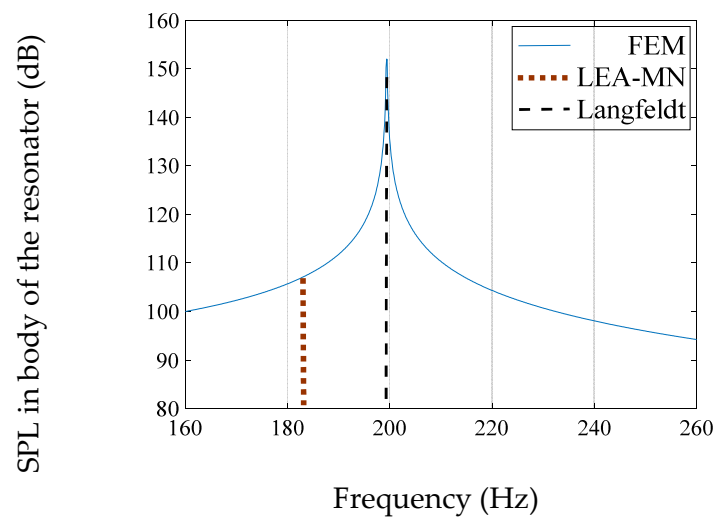


**Figure 10.** Solid line: sound pressure level in the body of the Helmholtz resonator calculated with FEM. Dotted line: resonance frequency calculated with lumped element approximation (multi-neck). Dashed line: resonance frequency calculated with Langfeldt et al.'s [33] formula.

#### 4.2.4. Cylindrical Body #2 (Different Necks)

In this case, a multi-neck Helmholtz resonator with a cylindrical body and two cylindrical necks with different dimensions was considered (Figure 11). The tube radius of the first neck was  $a = 0.01$  m and the tube length was  $L = 0.05$  m. The tube radius of the second neck was  $a/4$  and the tube length was  $L/4$ . Regarding the body of the resonator, the cylinder radius was 0.05 m and the cylinder height was 0.1 m. Using the FEM, the acoustic pressure in the Helmholtz resonator's volume was determined. Additionally, the resonance frequency was calculated according to the lumped-element approximation (multi-neck) and according to Langfeldt et al.'s [33] theoretical formulation. The resonance frequency calculated with the FEM was 161.3 Hz, with the lumped-element approximations (multi-neck) was 148.4 Hz and with the Langfeldt et al. [33] theoretical formulation was 161.0 Hz (Figure 12). Additionally, shown in Figure 11 are the acoustic pressure and sound pressure levels for the resonance frequency in the resonator's volume.

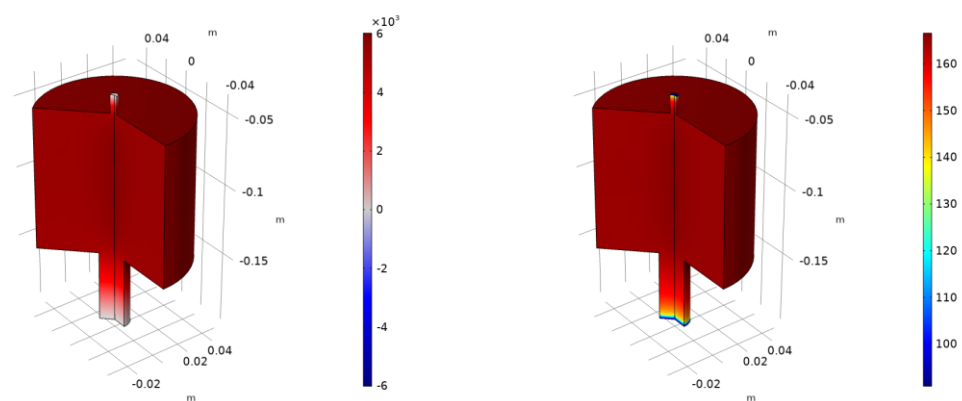


**Figure 11.** Acoustic pressure (left) (Pa) and sound pressure level (right) (dB) for the resonance frequency calculated with FEM (161.3 Hz).

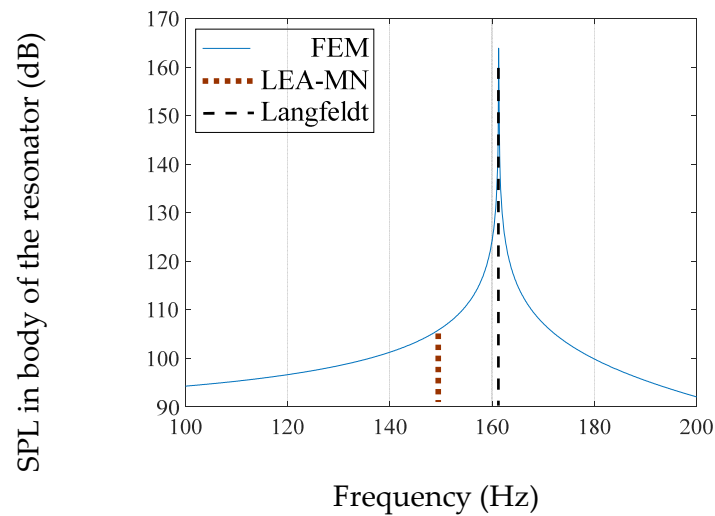


**Figure 12.** Solid line: sound pressure level in the body of the Helmholtz resonator calculated with FEM. Dotted line: resonance frequency calculated with lumped element approximation (multi-neck). Dashed line: resonance frequency calculated with Langfeldt et al.'s [33] formula.

#### 4.2.5. Cylindrical Body #3 (Different Necks, One Flanged Neck)

For this final case, a multi-neck Helmholtz resonator with a cylindrical body and two cylindrical necks with different dimensions was considered (Figure 13). The tube radius of the first neck was  $a = 0.01$  m and the tube length was  $L = 0.05$  m. The tube radius of the second neck was  $a/4$  and the tube length was  $L/100$ . The second neck is flanged for the resonator. Regarding the body of the resonator, the cylinder radius was 0.05 m and the cylinder height was 0.1 m. The acoustic pressure in the volume of the Helmholtz resonator was calculated with the FEM. In addition, the lumped-element approximation was used to obtain the resonance frequency (multi-neck) and also according to Langfeldt et al.'s [33] theoretical formulation. The resonance frequency calculated with the FEM was 248.5 Hz, with the lumped-element approximations (multi-neck) was 148.4 Hz and with the Langfeldt et al. [33] theoretical formulation was 245.7 Hz (Figure 14). Additionally, shown in Figure 13 are the acoustic pressure and sound pressure levels for the resonance frequency in the resonator's volume.

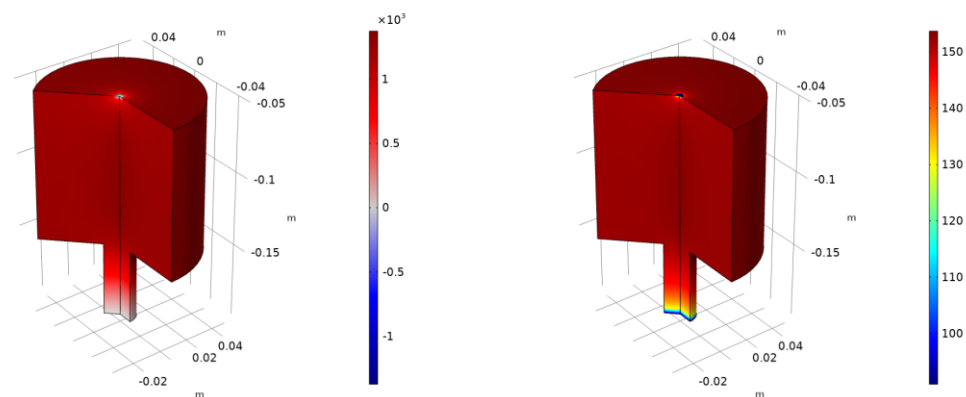


**Figure 13.** Acoustic pressure (left) (Pa) and sound pressure level (right) (dB) for the resonance frequency calculated with FEM (248.5 Hz).

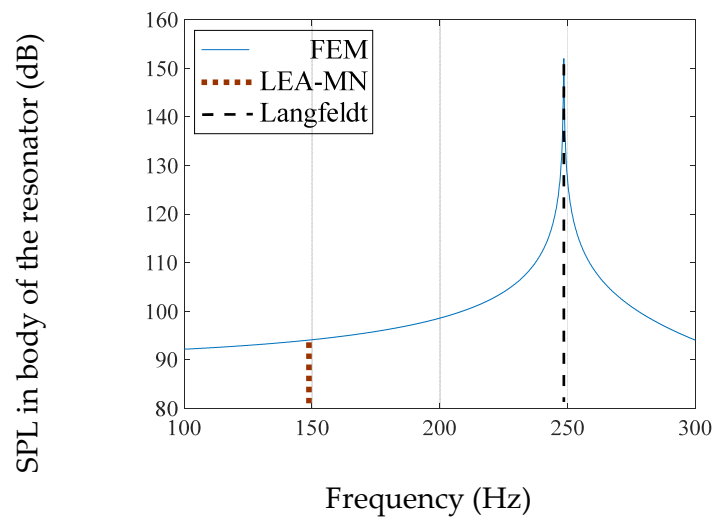


**Figure 14.** Solid line: sound pressure level in the body of the Helmholtz resonator calculated with FEM. Dotted line: resonance frequency calculated with lumped element approximation (multi-neck). Dashed line: resonance frequency calculated with Langfeldt et al.’s [33] formula.

**5. Discussion**

In the results section, the FEM results were compared with the results of Langfeldt et al.’s [33] theoretical formulation and with the outcome of the lumped element approximation in cases of single-neck and multi-neck Helmholtz resonators. Various cases of Helmholtz resonators were examined: with cylindrical or spherical bodies, with unflanged or flanged necks of various dimensions and with various combinations of the above.

A comparison of the results for the single-neck Helmholtz resonators between the FEM model and lumped-element approximation show very little deviation with an error of calculation less than 0.1% (Table 1). These findings are in line with research in the literature that demonstrate the effectiveness of the FEM in determining a (single-neck) Helmholtz resonator’s resonance frequency (e.g., [47]). The above is an indication that our single-neck models are structured correctly, behave as expected and are a good starting base for modeling the multi-neck Helmholtz resonators.

**Table 1.** Comparison of the results of the resonant frequency calculated with the lumped element approximation, with the Langfeldt formula and with FEM. Error of calculation is also presented.

	Resonant Frequency LEA (Hz)	Resonant Frequency Langfeldt (Hz)	Resonant Frequency FEM (Hz)	Error of Calculation (%) FEM-Langfeldt	Error of Calculation (%) FEM-LEA
<b>Single-neck models</b>					
Spherical	123.8	-	123.7	-	0.1
Cylindrical	144.0	-	144.0	-	0.0
<b>Multi-neck models</b>					
Spherical #1	249.4	249.4	249.7	0.1	0.1
Cylindrical #1	203.6	203.6	204.3	0.3	0.3
Spherical #2	181.8	197.1	199.3	1.1	8.8
Cylindrical #2	148.4	161.0	161.3	0.2	8.0
Cylindrical #3	148.4	245.7	248.5	1.1	40.3

For the multi-neck Helmholtz resonators, the overall results of the resonance frequency calculated with the FEM, the Langfeldt et al. [33] formula and lumped element approximation (multi-neck) are presented in Table 1. The error of calculation between the results of the FEM and Langfeldt et al.’s [33] formula, as well as the FEM and lumped element

approximation (multi-neck) is also presented. It is obvious that the addition of an extra neck causes the resonance frequency to increase, something that has also been observed in related studies [33,34].

A comparison of the results between the FEM and Langfeldt et al.'s [33] formula shows very small differences, which, in each case, has an error of calculation less than 1.1%. In contrast, a comparison of the results between the FEM and the lumped element approximation (multi-neck) shows significant differences which can reach up to a 40.3% error of calculation. This demonstrates that the lumped element approximation for multi-neck Helmholtz resonators is not suitable for the estimation of the resonance frequencies. The same was also pointed out by Selamet et al. [34] and Langfeldt et al. [33] that accounting for the other necks in the Helmholtz resonator by merely adding the aggregate surface area of the additional necks to that of the principal neck could not provide accurate results.

Therefore, the contribution of this research can be focused on two important areas. First, that the lumped element approximation for multi-neck Helmholtz resonators is not suitable for the estimation of the resonance frequencies in cases of multi-neck Helmholtz resonators as, in some cases, it can have a very large deviation. Secondly, the results of the FEM for the calculation of resonance frequency for multi-neck Helmholtz resonators have very small deviations from the results of the analytical method. This outcome is significant as the Langfeldt et al. [24] formula has been verified using experimental data. This, in turn, shows that the result of the FEM modeling is most likely to correspond to experimental results.

The ability of the FEM to estimate the resonance frequency of multi-neck Helmholtz resonators can be useful in many practical cases. An advantage of the FEM approach, similar to the analytical approach, is that it will be able to rapidly estimate the resonance frequency of the multi-neck Helmholtz resonators in contrast to the method by Selamet et al. [34]. The method is easily applicable and accessible using commercial software, in contrast to Selamet et al.'s [34] elaborate multi-dimensional boundary element model.

Another area of many practical applications depends on the ability of the FEM to be applied in cases with many different geometries, of which it is not trivial to apply the analytical formula of Langfeldt et al. [33]. As presented in the introduction, there are many different variations of the resonator's neck form (e.g., spiral neck [26], tapered neck [27], extended neck [28], angled neck aperture [29]) or possibly a combination of those. Applying the FEM in these cases can provide results that are difficult to achieve in other ways. The same applies in cases where there may be various combinations between the neck and the body of the resonator (e.g., neck-cavity-neck-cavity [32]). In such cases, due to the complex geometry, the FEM is a realistic approach for the estimation of the resonance frequency. In addition, the same applies in cases where manufacturing tolerances makes it impossible to prevent leaks or gaps in Helmholtz resonators in many real-world applications [34], which are sometimes even necessary, e.g., to allow drainage of moisture accumulating inside the cavity [36].

To establish the method's efficiency over a wide range of cases, more research must be conducted. The present study has only investigated a limited number of cases of multi-neck Helmholtz resonators. However, this study has gone some way towards enhancing our understanding of the applicability of the FEM for the estimation of the resonance frequency of multi-neck Helmholtz resonators. Future work is already underway for the application of the FEM to a broader range of cases.

## 6. Conclusions

For this study, the FEM was employed for the estimation of the resonance frequency of a Helmholtz resonator with multiple necks. Various cases of multi-neck Helmholtz resonators were examined: with cylindrical or spherical bodies, with unflanged or flanged necks of various dimensions and with various combinations of the above, as well as single neck resonators. The FEM results were compared with the results of Langfeldt et al.'s [33] theoretical formulation and with the outcome of the lumped element approximation (multi-

neck), accounting for the added neck surface area. Comparisons revealed little deviation between the FEM and theoretical model (less than 1.1% error of calculation for every case). On the contrary, in comparison with the lumped element approximation (multi-neck), the error of calculation was significant (up to 40.3% for the cases examined). The results from this study point towards the idea that the FEM is effective for the calculation of the resonance frequency in the case of multi-neck Helmholtz resonators. We have obtained satisfactory results demonstrating that an application of the FEM can be effective in a variety of cases.

The present study has only investigated a limited number of multi-neck Helmholtz resonator cases. Further work needs to be carried out to establish the generalizability of the effectiveness of the FEM for modeling the resonances of multi-neck Helmholtz resonators. However, our results are encouraging and should be validated by a larger sample size. This approach will prove useful in expanding our understanding of how multi-neck Helmholtz resonators operate. Future studies should concentrate on the performance of multi-neck Helmholtz resonators under various conditions and configurations where analytical solutions are difficult to implement (e.g., different neck configurations). This approach could be applied in various fields such as acoustic metamaterials, musical acoustics and noise mitigation. We hope that our research will serve as a base for future studies on this issue.

**Author Contributions:** Conceptualization, N.M.P. and G.E.S.; methodology, N.M.P.; software, N.M.P.; validation, N.M.P. and G.E.S.; formal analysis, N.M.P. and G.E.S.; investigation, N.M.P. and G.S.; resources, N.M.P.; data curation, N.M.P. and G.E.S.; writing—original draft preparation, N.M.P.; writing—review and editing, G.E.S.; visualization, N.M.P.; supervision, G.E.S.; project administration, N.M.P. and G.E.S. All authors have read and agreed to the published version of the manuscript.

**Funding:** This research received no external funding.

**Institutional Review Board Statement:** Not applicable.

**Informed Consent Statement:** Not applicable.

**Data Availability Statement:** The data presented in this study are available on request from the corresponding author.

**Conflicts of Interest:** The authors declare no conflict of interest.

## References

1. Rossing, T.D.; Rossing, T.D. *Springer Handbook of Acoustics*; Springer: Berlin/Heidelberg, Germany, 2014.
2. Crocker, M.J.; Price, A.J. *Noise and Noise Control: Volume 1*; CRC Press: Boca Raton, FL, USA, 2018.
3. Kone, C.T.; Ghinet, S.; Panneton, R.; Dupont, T.; Grewal, A. Multi-tonal low frequency noise control for aircraft cabin using Helmholtz resonator with complex cavity designs for aircraft cabin noise improvement. In Proceedings of the INTERNOISE-2021, virtually, 1–5 August 2021.
4. Zhang, Z.; Yu, D.; Liu, J.; Hu, B.; Wen, J. Transmission and bandgap characteristics of a duct mounted with multiple hybrid Helmholtz resonators. *Appl. Acoust.* **2021**, *183*, 108266. [[CrossRef](#)]
5. Wu, C.; Chen, L.; Ni, J.; Xu, J. Modeling and experimental verification of a new muffler based on the theory of quarter-wavelength tube and the Helmholtz muffler. *SpringerPlus* **2016**, *5*, 1–14. [[CrossRef](#)] [[PubMed](#)]
6. Wang, J.; Rubini, P.; Qin, Q.; Houston, B. A model to predict acoustic resonant frequencies of distributed Helmholtz resonators on gas turbine engines. *Appl. Sci.* **2019**, *9*, 1419. [[CrossRef](#)]
7. Kanev, N. Maximum sound absorption by a Helmholtz resonator in a room at low frequencies. *Acoust. Phys.* **2018**, *64*, 774–777. [[CrossRef](#)]
8. Herrero-Durá, I.; Cebrecos, A.; Picó, R.; Romero-García, V.; García-Raffi, L.M.; Sánchez-Morcillo, V.J. Sound absorption and diffusion by 2D arrays of Helmholtz resonators. *Appl. Sci.* **2020**, *10*, 1690. [[CrossRef](#)]
9. Papadakis, N.M.; Stavroulakis, G.E. Review of Acoustic Sources Alternatives to a Dodecahedron Speaker. *Appl. Sci.* **2019**, *9*, 3705. [[CrossRef](#)]
10. Papadakis, N.M.; Stavroulakis, G.E. Handclap for Acoustic Measurements: Optimal Application and Limitations. *Acoustics* **2020**, *2*, 224–245. [[CrossRef](#)]
11. Papadakis, N.M.; Stavroulakis, G.E. Low Cost Omnidirectional Sound Source Utilizing a Common Directional Loudspeaker for Impulse Response Measurements. *Appl. Sci.* **2018**, *8*, 1703. [[CrossRef](#)]
12. Papadakis, N.M.; Antoniadou, S.; Stavroulakis, G.E. Effects of Varying Levels of Background Noise on Room Acoustic Parameters, Measured with ESS and MLS Methods. *Acoustics* **2023**, *5*, 563–574. [[CrossRef](#)]

13. Kanev, N. Resonant Vessels in Russian Churches and Their Study in a Concert Hall. In Proceedings of the Acoustics, Virtual, 5–9 October 2020; pp. 399–415.
14. Pöhlmann, E. Vitruvius De Architectura V: Resounding Vessels in the Greek and Roman Theatre and Their Possible Afterlife in Eastern and Western Churches. *Greek Rom. Music. Stud.* **2021**, *9*, 157–174. [[CrossRef](#)]
15. Fredianelli, L.; Del Pizzo, L.G.; Licitra, G. Recent developments in sonic crystals as barriers for road traffic noise mitigation. *Environments* **2019**, *6*, 14. [[CrossRef](#)]
16. Castiñeira-Ibañez, S.; Rubio, C.; Sánchez-Pérez, J.V. Environmental noise control during its transmission phase to protect buildings. Design model for acoustic barriers based on arrays of isolated scatterers. *Build. Environ.* **2015**, *93*, 179–185. [[CrossRef](#)]
17. Redondo, J.; Ramírez-Solana, D.; Picó, R. Increasing the Insertion Loss of Sonic Crystal Noise Barriers with Helmholtz Resonators. *Appl. Sci.* **2023**, *13*, 3662. [[CrossRef](#)]
18. Garcia-Alcaide, V.; Palleja-Cabre, S.; Castilla, R.; Gamez-Montero, P.J.; Romeu, J.; Pamies, T.; Amate, J.; Milán, N. Numerical study of the aerodynamics of sound sources in a bass-reflex port. *Eng. Appl. Comput. Fluid Mech.* **2017**, *11*, 210–224. [[CrossRef](#)]
19. Nia, H.T.; Jain, A.D.; Liu, Y.; Alam, M.-R.; Barnas, R.; Makris, N.C. The evolution of air resonance power efficiency in the violin and its ancestors. *Proc. R. Soc. A Math. Phys. Eng. Sci.* **2015**, *471*, 20140905. [[CrossRef](#)]
20. Yamamoto, T. Acoustic metamaterial plate embedded with Helmholtz resonators for extraordinary sound transmission loss. *J. Appl. Phys.* **2018**, *123*, 215110. [[CrossRef](#)]
21. Casarini, C.; Tiller, B.; Mineo, C.; MacLeod, C.N.; Windmill, J.F.; Jackson, J.C. Enhancing the sound absorption of small-scale 3-D printed acoustic metamaterials based on Helmholtz resonators. *IEEE Sens. J.* **2018**, *18*, 7949–7955. [[CrossRef](#)]
22. Yang, X.; Yin, J.; Yu, G.; Peng, L.; Wang, N. Acoustic superlens using Helmholtz-resonator-based metamaterials. *Appl. Phys. Lett.* **2015**, *107*, 193505. [[CrossRef](#)]
23. Fang, N.; Xi, D.; Xu, J.; Ambati, M.; Srituravanich, W.; Sun, C.; Zhang, X. Ultrasonic metamaterials with negative modulus. *Nat. Mater.* **2006**, *5*, 452–456. [[CrossRef](#)] [[PubMed](#)]
24. Ciaburro, G.; Iannace, G. Numerical simulation for the sound absorption properties of ceramic resonators. *Fibers* **2020**, *8*, 77. [[CrossRef](#)]
25. Yuan, M.; Cao, Z.; Luo, J.; Chou, X. Recent developments of acoustic energy harvesting: A review. *Micromachines* **2019**, *10*, 48. [[CrossRef](#)]
26. Shi, X.; Mak, C.M. Helmholtz resonator with a spiral neck. *Appl. Acoust.* **2015**, *99*, 68–71. [[CrossRef](#)]
27. Tang, S.K. On Helmholtz resonators with tapered necks. *J. Sound Vib.* **2005**, *279*, 1085–1096. [[CrossRef](#)]
28. Cai, C.; Mak, C.-M.; Shi, X. An extended neck versus a spiral neck of the Helmholtz resonator. *Appl. Acoust.* **2017**, *115*, 74–80. [[CrossRef](#)]
29. Ramos, D.; Godinho, L.; Amado-Mendes, P.; Mareze, P. Experimental and numerical modelling of Helmholtz Resonator with angled neck aperture. In Proceedings of the INTER-NOISE and NOISE-CON Congress and Conference Proceedings, Virtual, 16–20 November 2020; pp. 37–47.
30. Chanaud, R. Effects of geometry on the resonance frequency of Helmholtz resonators, part I. *J. Sound Vib.* **1994**, *178*, 337–348. [[CrossRef](#)]
31. Chanaud, R. Effects of geometry on the resonance frequency of Helmholtz resonators, part II. *J. Sound Vib.* **1997**, *204*, 829–834. [[CrossRef](#)]
32. Xu, M.; Selamet, A.; Kim, H. Dual helmholtz resonator. *Appl. Acoust.* **2010**, *71*, 822–829. [[CrossRef](#)]
33. Langfeldt, F.; Hoppen, H.; Gleine, W. Resonance frequencies and sound absorption of Helmholtz resonators with multiple necks. *Appl. Acoust.* **2019**, *145*, 314–319. [[CrossRef](#)]
34. Selamet, A.; Kim, H.; Huff, N.T. Leakage effect in Helmholtz resonators. *J. Acoust. Soc. Am.* **2009**, *126*, 1142–1150. [[CrossRef](#)]
35. Lee, I.; Jeon, K.; Park, J. The effect of leakage on the acoustic performance of reactive silencers. *Appl. Acoust.* **2013**, *74*, 479–484. [[CrossRef](#)]
36. May, D.; Plotkin, K.; Selden, R.; Sharp, B. *Lightweight Sidewalls for Aircraft Interior Noise Control*; National Aeronautics and Space Administration: Washington, DC, USA, 1985.
37. Zolfagharian, A.; Noshadi, A.; Khosravani, M.R.; Zain, M.Z.M. Unwanted noise and vibration control using finite element analysis and artificial intelligence. *Appl. Math. Model.* **2014**, *38*, 2435–2453. [[CrossRef](#)]
38. Sakuma, T.; Sakamoto, S.; Otsuru, T. *Computational Simulation in Architectural and Environmental Acoustics*; Springer: Berlin/Heidelberg, Germany, 2014.
39. Papadakis, N.M.; Stavroulakis, G.E. Finite Element Method for the Estimation of Insertion Loss of Noise Barriers: Comparison with Various Formulae (2D). *Urban Sci.* **2020**, *4*, 77. [[CrossRef](#)]
40. Papadakis, N.M.; Stavroulakis, G.E. Time domain finite element method for the calculation of impulse response of enclosed spaces. Room acoustics application. In Proceedings of the Mechanics of Hearing: Protein to Perception: 12th International Workshop on the Mechanics of Hearing, Cape Sounio, Greece, 31 December 2015; Volume 1703, p. 100002. [[CrossRef](#)]
41. Beranek, L.L.; Mellow, T. *Acoustics: Sound Fields and Transducers*; Academic Press: Cambridge, MA, USA, 2012.
42. Ingard, U. *Notes on acoustics*; Laxmi Publications, Ltd.: Delhi, India, 2010.
43. Kuttruff, H. *Room Acoustics*; CRC Press: Boca Raton, FL, USA, 2016. [[CrossRef](#)]
44. Crocker, M.J.; Arenas, J.P. *Engineering Acoustics: Noise and Vibration Control*; John Wiley & Sons: Hoboken, NJ, USA, 2021.

45. Marburg, S.; Nolte, B. *Computational Acoustics of Noise Propagation in Fluids: Finite and Boundary Element Methods*; Springer: Berlin/Heidelberg, Germany, 2008; Volume 578.
46. Blackstock, D.T. *Fundamentals of Physical Acoustics*; Wiley: Hoboken, NJ, USA, 2001.
47. Jena, D.; Dandsena, J.; Jayakumari, V. Demonstration of effective acoustic properties of different configurations of Helmholtz resonators. *Appl. Acoust.* **2019**, *155*, 371–382. [[CrossRef](#)]
48. Ihlenburg, F. *Finite Element Analysis of Acoustic Scattering*; Springer Science & Business Media: Berlin/Heidelberg, Germany, 2006; Volume 132.

**Disclaimer/Publisher’s Note:** The statements, opinions and data contained in all publications are solely those of the individual author(s) and contributor(s) and not of MDPI and/or the editor(s). MDPI and/or the editor(s) disclaim responsibility for any injury to people or property resulting from any ideas, methods, instructions or products referred to in the content.